Fluid-structure interaction during wave-impact with air-entrapment in a sloshing tank.

C. Lugni[*,**] claudio.lugni@cnr.it *A. Bardazzi*[***] bardazzi.andrea@gmail.com

O. M. Faltinsen[**] oddfal@marin.ntnu.no *G. Graziani*[***] g.graziani@uniroma1.it

∗ CNR-INSEAN, National Research Council, Roma – Italy.
∗∗ Centre for Autonomous Marine Operations and Systems, NTNU, Trondheim – Norway.
∗ ∗ ∗ Dipartimento DIMA, Universita' degli studi di Roma 'Sapienza'.

The investigation carried out in the present research pursues the study started several years ago about the wave-impact phenomena in a sloshing tank relevant for a Liquefied Natural Gas ship at low filling depth. Depending on the local features of the wave approaching the tank wall, different impact phenomena may occur. When the angle between the liquid and the wall is small, a single gas bubble is entrapped during the impact; differently, for larger angle of impact, flip-through event or flat-impact may occur. Previous investigations for a fully 2D rigid tank [(1), (2), (3)], emphasized that the maximum pressure along the wall is not a reliable indicator of the maximum load, because of the stochastic nature of the local flow which characterizes the slamming phenomena. Further, when gas-entrapment matters making important the compressibility of the gas and its interaction with the free surface, Euler and Cavitation numbers, in addition to the traditional Froude scaling, should be taken into account for a proper scaling of the maximum loads [(2), (3)].

Based on the above results, in the last year new physical effects have been investigated by the present research group by means of a hydroelastic study. Hydroelasticity indeed, may be a crucial issue when slamming events occur in a LNG tank. Because of the low temperature inside the tank used to ensure the liquid state of the gas, the side walls, designed to realize a good thermal insulation, are not able to support the buffles traditionally installed in oil tankers to damp the sloshing phenomena. Then violent impacts may happen, especially in low filling conditions, when a travelling bore or an incipient breaking wave approaching the wall may characterize the sloshing flow inside the tank (4). These events, localized in space and time, may compromise the integrity of the structure when the time scales of the impacts are comparable to the highest natural vibration period of the structure. In this case hydroelasticity matters, as testified in previous experimental studies (5), (6) focused on the evolution of the flip-through event and an hybrid numerical-experimental hydroelastic model has been proposed to assess the relevance of hydroelasticity.

Here, an experimental investigation is presented to study the role of the hydroelasticity during the evolution of a slamming event with air-entrapment. The strain distribution along a deformable aluminum plate inserted in a rigid vertical wall of a sloshing tank has been measured to characterize the features of the local loads. Depressurized conditions have been realized to examine the relevance of the Euler and Cavitation numbers on the hydroelasticity of the deformable wall.

The same setup used in (5), (6) has been applied in the present experiments. A 2D plexiglas tank (LxHx$B = 1$ m x 1 m x 0.1 m) reinforced with steel and aluminum structure has been used to allow tests in depressurized conditions (see fig. 1). A filling depth $h/L = 0.122$ has been considered. An elastic aluminum plate, whose lowest natural wet frequency (in fully wet condition) has been Froude-scaled with respect to that of the typical panel used in a Mark III containment system (4), has been inserted in an extremely rigid stainless steel wall. The plate, 9 cm high, $2,5$ mm thick and located at 13 cm from the bottom of the tank, corresponds to a scale factor 30. It is clamped to the steel frame in correspondence to the vertical ends, while the lateral boundaries are left free. In this way, assuming a two-dimensional evolution of the hydrodynamic load, a double-clamped beam behaviour is realized. In depressurized conditions, in order to ensure the same ullage pressure on the rear (looking outside the tank, i.e. in air) and on the front (looking inside the tank, i.e. in water) side of the plate, an *ad hoc* small steel tank has been built (see bottom-left image on fig. 1) and fixed rigidly to the main sloshing tank. The small tank has been connected to the same vacuum pump used to realize the depressurized conditions in the main tank; in this way, ullage pressure has been decreased from atmospheric pressure down to 25 mbar. Finally, the hexapod system 'MISTRAL' (made by Symetrie) forced a pure sway sinusoidal motion of the tank. The measurement setup for the hydroelastic investigation was composed by two differential pressure probes along the rigid vertical wall below the elastic plate and five strain gauges along the deformable aluminum plate (see top panel on figure 1). Preliminarily, aiming to determine the dynamic response of the strain gauges, two miniaturized accelerometers have been mounted next to two strain gauges and the corresponding signals have been compared.

A second setup is used to ensure the repeatability of the flow conditions in the fully rigid case (no hydroelastic case). To the aim, the thin elastic plate is substituted with a rigid aluminum plate 20 mm thick. An accelerometer is put on the vertical rigid wall to check its rigidity as well as the global motion of the tank. Five differential pressure transducers were mounted along the rigid plate at the same positions of the strain gauges in the elastic case. The signals of the transducers were recorded through an acquisition system with a sample rate of 50 kHz. During the tests, visualizations of the local flow during the evolution of the phenomenon were performed through a high-speed digital video camera (with sample rate of 5 kHz), while a global view of the sloshing flow was recorded through two slow digital cameras (with a sample rate

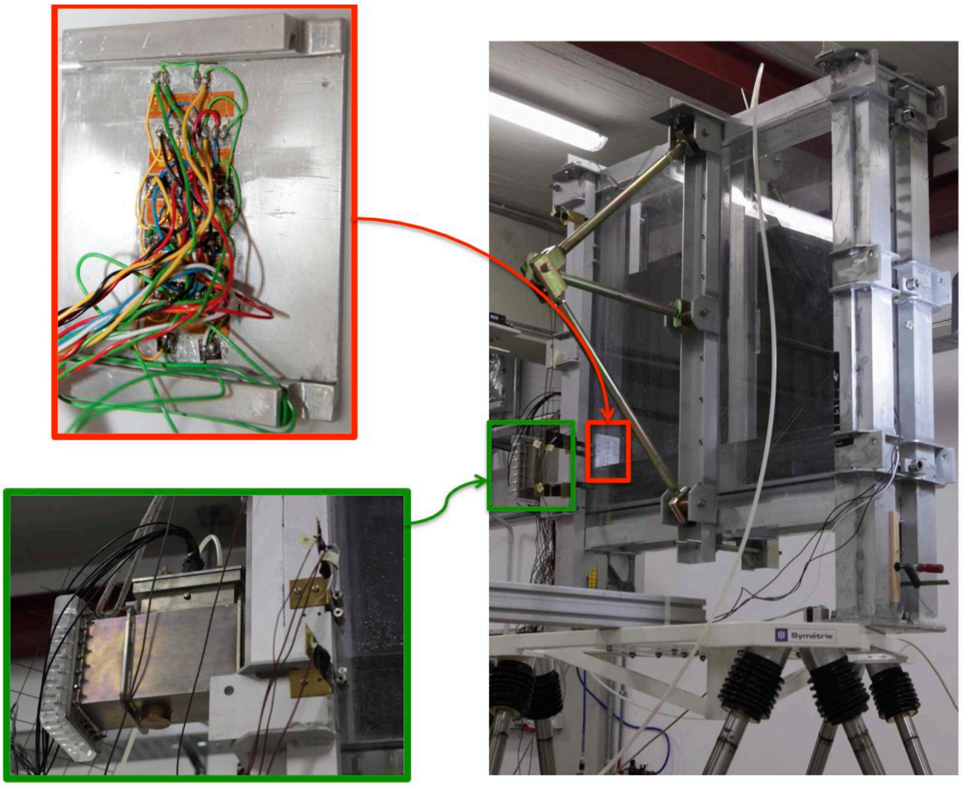

Figure 1:
Experimental set-up for the sloshing-tank experiments. Top-left panel: enlarged view of the rear part of the elastic plate with the strain gauges (top panel). Bottom-left panel: enlarged view of the small tank used to ensure the depressurized conditions on the external part of the elastic plate.

of 100 Hz). A common reference signal was used to synchronize the images with the analog signals of the transducers. Finally, an absolute pressure transducer measured the ullage pressure inside the tank.

Some preliminary results. The same impact scenario, that is a wave impact with air entrapped at the wall, is realized experimentally imposing a sinusoidal motion of the tank with period equal to 1.6 s. Three different sizes of the entrapped air-cavity, large (case a)), medium (case b)) and small (case c)), are investigated by changing the amplitude of the sinusoidal motion, i.e. 65 mm, 63 mm and 61.5 mm, respectively. The influence of the Euler number, i.e. of the ullage pressure inside the tank, has been investigated. In the following, some preliminary results will be discussed, postponing to the Workshop the complete analysis of the investigation.

Figures 2, 3 and 4 show the time history of the strain measured by the gauge placed in the centre of the elastic plate, for the large, medium and small air-cavity case, respectively. Each figure from left to right reports three different panels corresponding to three different values of the ullage pressure: 100 mbar, 400 mbar and 800 mbar, respectively. According to the study performed in (3) for a fully rigid tank, the oscillation frequency of the air-cavity depends on the Euler number, increasing with the ullage pressure of the tank. However, when an elastic plate is considered, the structural natural frequency may be excited as well. The last event depends on the time rise of the first peak of the hydrodynamic load. Of course, when the frequency of the bubble is close to the natural structural frequency, a resonance phenomenon is expected. Although a really small air-cavity has been obtained for the case c), its highest frequency of oscillation (occurring at atmospheric pressure) is still slightly smaller than the lowest natural frequency of the structure.

In correspondence of the lowest ullage pressure (see left panel of each figure), the two frequencies, i.e. that of the bubble and the lowest natural frequency of the structure, are expected to be quite far from each other. Indeed, the first one decreases with the Euler number, while the second one, though dependent on the wetted length of the deformable plate is practically Euler number independent (neglecting the small variation induced by the different wetted length due to the different size of the cavity with the Euler number). This mechanism justifies the strain time history observed on the left panel of the figures 2-3-4. More in detail, the time rise of the first peak is able to excite the hydroelastic behavior of the elastic plate, as highlighted by the vibration (around 1 kHz) occurring during the first 6 ms. However, for the case a) the larger time rise characterizing the first peak (about 2 ms) is not enough to excite a relevant hydroelastic phenomenon. Further, as expected for the lowest ullage pressure case, the hydroelastic frequency is much larger than the oscillation frequency of the air-cavity; this means that during the first oscillation of the bubble (i.e. 12 ms, 9 ms and 6 ms for the case a, b and c, respectively) the hydroelastic vibrations are completely damped out. When increasing the ullage pressure (see middle and right panels of figures 2-3-4), the oscillation frequency of the air-cavity increases, approaching the lowest natural frequency. This phenomenon causes a different behavior for the case a), b) and c): while the maxima and minima of the strains are almost the same of the large bubble case, they vary consistently (but for the first peak) for the medium and small bubble cases. A possible reason of this behavior could be the interaction between the vibration of the structure and the oscillation of the bubble. However, at the moment it is premature to draw any definitive conclusion. Note, finally, that for each of the three cases considered, the value of the first peak of the strain remains almost unchanged with the Euler number. This suggests that this peak is not dominated by the compressibility of the air-cavity.

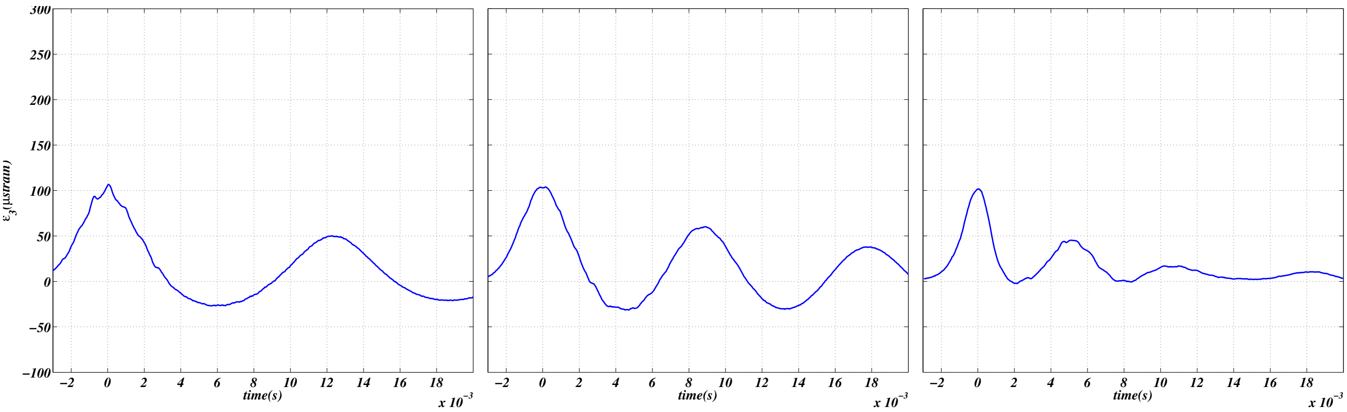

Figure 2: Case a. Large air-cavity entrapped. From left to right: time history of the strain measured at the centre of the elastic plate, for three different values of the ullage pressure (100 mbar, 400 mbar and 800 mbar, respectively).

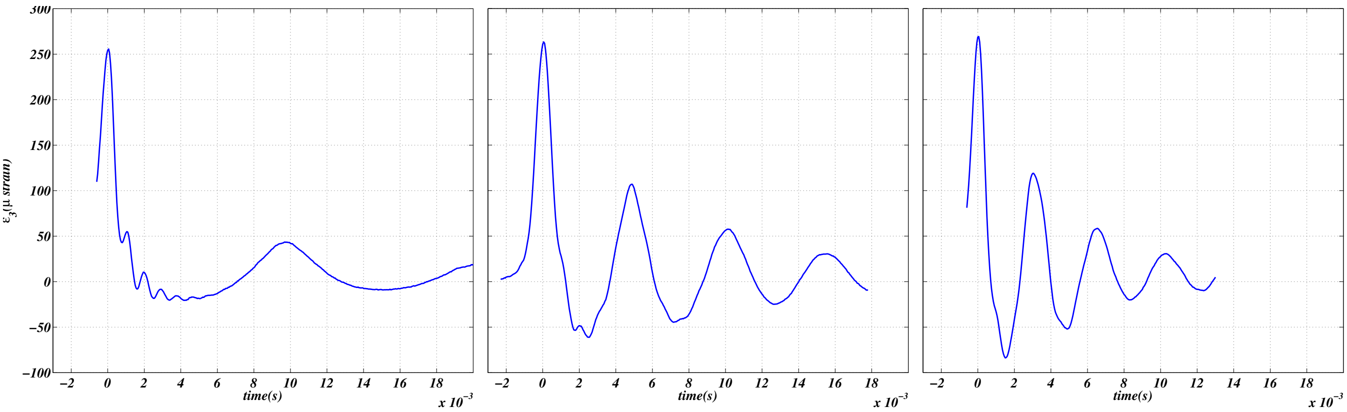

Figure 3: Case b. Medium air-cavity entrapped. From left to right: time history of the strain measured at the centre of the elastic plate, for three different values of the ullage pressure (100 mbar, 400 mbar and 800 mbar, respectively).

This research activity was partially supported by the Centre for Ships and Ocean Structures (CeSOS), NTNU, Trondheim, within the ”Violent Water-Vessel Interactions and Related Structural Loads” project and presently ongoing within the new born Centre for Autonomous Marine Operations and Systems (AMOS), Trondheim, and partially funded by the Flagship Project RITMARE - The Italian Research for the Sea - coordinated by the Italian National Research Council and funded by the Italian Ministry of Education, University and Research within the National Research Program 2011-2013.”

References

[1] C. Lugni, M. Brocchini, and O. M. Faltinsen, “Wave impact loads: The role of flip-through,” *Physics of Fluids*, no. 18, p. 19, 2006.

[2] C. Lugni, M. Miozzi, M. Brocchini, and O. M. Faltinsen, “Evolution of the air cavity during a depressurized wave impact.i. the kinematic flow field,” *Physics of Fluids*, no. 22, p. 16, 2010.

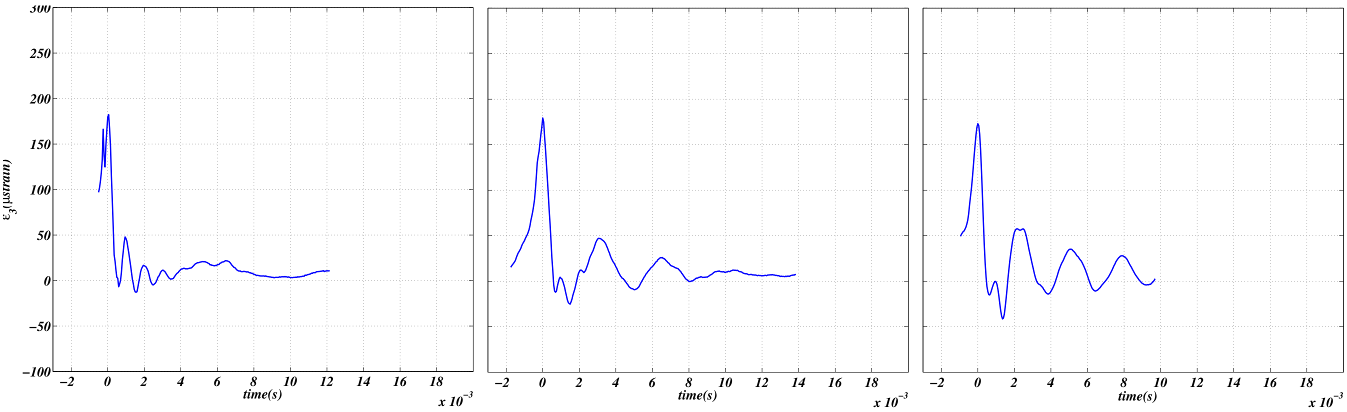

Figure 4: Case c. Small air-cavity entrapped. From left to right: time history of the strain measured at the centre of the elastic plate, for three different values of the ullage pressure (100 mbar, 400 mbar and 800 mbar, respectively).

[3] C.Lugni, M.Brocchini, and O. Faltinsen, "Evolution of the air cavity during a depressurized wave impact.ii. the dynamic field," *Physics of Fluids*, no. 22, p. 13, 2010.

[4] O. M. Faltinsen and A. N. Timokha, *Sloshing*. Cambridge, UK: Cambridge University Press, 2010.

[5] A. Bardazzi, C. Lugni, O. Faltinsen, M. Greco, G. Colicchio, and G. Graziani, "Wave-impact in a sloshing tank: hydroelastic challenges," *Proc. IWWWFB, Denmark*, 2012.

[6] A. Bardazzi, C. Lugni, O. Faltinsen, and G. Graziani, "Hydroelastic study of the impact phenomena in sloshing flow," *Hydroelasticity in Marine Technology, Tokyo*, 2012.